Mon. Not. R. Astron. Soc. **272**, 61–70 (1995)

Effect of gas drag on the dynamics of protostellar clumps in molecular clouds

U. Gorti and H. C. Bhatt

Indian Institute of Astrophysics, Koramangala, Bangalore 560034, India

Accepted 1994 August 1. Received 1994 July 20; in original form 1994 March 7

ABSTRACT

Molecular clouds are observed to have substructure within them, and to consist of dense condensations or clumps which are surrounded by a less-dense interclump medium. The interclump gas could retard the motion of the clumps in the cloud through a drag force caused by dynamical friction. The effect of such a drag force on the dynamics of protostellar clumps in a molecular cloud is numerically analysed in this paper. As the dynamical drag acting on a clump is dependent on its mass, clumps of different masses have, in general, different retardations. It is found that the most massive objects suffer the maximum decelerating effects and settle to the centre in a shorter time than do the lower mass clumps. Thus there is a clustering of the clumps towards the centre of the cloud, and a radial segregation of mass is established in the cloud. The time-scale of the process is governed by the cloud parameters, and is shorter for denser clouds. The most massive protostellar clumps in the cloud are thus expected to lie at the centre of the cloud. The mass segregation observed in many young clusters of pre-main-sequence stars could be a result of dynamical drag.

Key words: methods: numerical – stars: formation – ISM: clouds – ISM: kinematics and dynamics.

1 INTRODUCTION

Molecular clouds form an important component of the interstellar medium in our Galaxy, and contain a significant amount of the total mass of interstellar gas. They cover a range of masses and sizes, varying from the large giant molecular cloud (GMC) complexes with masses of the order of 10^6 $M_\odot$ and sizes of 60 pc (e.g. W3 and M17) to the smallest dark clouds of masses ~ 10 $M_\odot$ and sizes of a few tenths of a parsec (e.g. TMC1 and the main core of B1). Observational studies of molecular clouds in the Galaxy, and especially in the solar neighbourhood, reveal a host of characteristic features, the most significant of which is that all star formation appears to take place in molecular clouds. Molecular clouds are gravitationally bound, and their masses typically exceed the Jeans mass by up to an order of magnitude. Not all molecular clouds are star formation sites, however, and even those that do form stars do not do so efficiently, converting only a small fraction of their mass into a stellar form. Any meaningful investigation of the star formation process must begin with an understanding of the molecular clouds – their structure, dynamics and evolution. It has long been known that molecular clouds have substructure within them, as large-scale maps and interferometric observations in the radio and millimetre-wave regions reveal clumpy structures within the clouds on all observable scale-sizes, from a few hundredths of a parsec to tens of parsecs (see e.g. Wilson & Walmsley 1989). The gas distribution is highly non-uniform, with spatially separated dense condensations in a ubiquitous less dense medium (e.g. Bally et al. 1987). However, the exact physical nature of these 'clumps' is as yet uncertain. They have been interpreted as temporary fluctuations in density caused by supersonic turbulence within the cloud (Falgarone & Phillips 1990; Scalo 1990). This view is supported by the apparent fractal nature of molecular clouds, which seem to show the same structure on smaller scales, traced by high-density tracers and high-resolution observations (Falgarone, Phillips & Walker 1991). The other interpretation is that the clumps represent stable physical entities, as they are well separated in position and velocity space as observed by molecular line spatial maps and velocity channel maps or position–velocity diagrams (see Blitz & Stark 1986; Stutzki & Güsten 1990). The large density contrast between the clumps and the medium in between them, and the observations of the association of young stellar objects with dense clump cores (Beichman et al. 1986; Tatematsu et al. 1993), favours the notion of clumps being distinct physical objects. Here, we adopt the latter view that these clumpy structures are actual mass concentrations. The densest of these structures (the protostellar clumps), upon gravitational collapse, would in fact give rise to the formation of stars. The existence of an 'interclump medium', or ICM, is inferred from the broad linewings on CO maps. The interclump medium is believed to consist of both molecular and atomic hydrogen, as evidenced by the presence of H I envelopes around GMCs, in varying fractions in different clouds (e.g. Blitz 1991). The nature of the ICM is not clear, however, and it may consist of a relatively homogeneous substrate or may also be clumpy with small density enhancements (Falgarone et al. 1991). Here we assume that the ICM is homogeneous on length-scales smaller than the clump size. Observations of both the warm GMCs (e.g. Orion A, B) and the cold dark clouds (e.g. Taurus) indicate that star-forming regions are often found to be in the close vicinity of the dense cloud cores, suggesting that stars form in the most dense areas of molecular clouds (Myers 1987; Lada 1990). The density contrast between the clumps and the ambient interclump medium is found to vary from cloud to cloud. Clouds that form massive O- and B-type stars, i.e. the warm and dense clouds, have a large clump-to-interclump density contrast, while the contrast is smaller for the low-mass star-forming dark clouds (Blitz & Stark 1986; Falgarone & Puget 1988). Observations seem to imply a ratio of about 10 to 100 for most clouds, and it appears that molecular clouds consist of self-gravitating clumps with a relatively large density compared to the surrounding medium. As clumps or possibly substructures within them seem to be the immediate precursors of stars, or, at the least, active star formation sites within the molecular clouds, a complete understanding of star formation and associated features (such as the initial mass function, and the rates and efficiency of star formation in galaxies) can be achieved only through a study of molecular clouds on all levels of the hierarchy, from the huge complexes to the smallest cores, and the physical processes that determine their evolution. The dynamical evolution of the clumpy structures in molecular clouds is of special relevance to the spatial aspects of the star formation process, as stars presumably form here and are affected directly by the dynamical history of the clumps/cores from which they form.

The CO linewidths in molecular clouds are invariably larger than the thermal linewidths, implying supersonic velocities which are typically of the order of a few km s^{-1} (e.g. Blitz 1991). Observations indicate that clouds on large scales are in virial equilibrium, and the larger clumps within them satisfy various scaling laws, such as mass–size ($M \propto R^2$), density–size ($\rho \propto R^{-1}$) and size–velocity dispersion ($\Delta v \propto R^{0.5}$) laws (e.g. Larson 1982; Elmegreen 1985). However, the more dense protostellar clumps that are gravitationally bound would be more compact than these scaling laws indicate.

The motion of the clumps through the interclump medium has potentially interesting consequences, brought about by the interaction of the dense condensations with the ambient gas. The clumps may accrete matter from the gas while moving through it, and also experience drag forces which decelerate them. The effect of drag due to dynamical friction on newly formed stars, while still embedded in their parent clump(s), has been discussed qualitatively by Bally & Lada (1991). They suggest that, in very dense massive cores of clouds, stars moving through the gas could cause 'cluster compactification' on a cloud crossing time-scale, leading to locally greater concentration of mass in stars.

In the present work, we have carried out a detailed numerical investigation of the effects of dynamical friction on the motion of dense protostellar clumps in molecular clouds. In addition to the frictional forces, the gravitational potential due to the gas and the clump–clump interactions have been included. Physical parameters of molecular clouds, such as size, mass, density, temperature, etc., have been chosen to agree with their observed values. Dynamical friction acting on a clump causes a deceleration which depends on the mass of the clump, as a result of the gravitational origin of the force, and hence the dynamics of the clumps are likely to depend on their masses. Consequently, mass segregation is established in the cloud, with a tendency for the more massive clumps to be located more centrally with respect to the cloud. The time evolution of such a cloud system will reflect its physical properties, and may also affect physical processes occurring in the cloud. The mass spectrum of clouds and clumps is observed to follow a power law ($dN/dM \propto M^{-x}$, where dN is the number of objects with mass between M and $M+dM$) over a range of masses spanning more than five orders of magnitude, with the index x varying from about 1.1 to 1.7 in various cases (Genzel 1992). Clumps undergoing collapse and on their way to forming stars may have steeper mass spectra, with a final stellar mass spectrum index of 2.35 (the Salpeter value). We have varied the power-law exponent within this range, and investigated any possible dependence of the dynamics of the system on the mass spectrum. Apart from dynamical effects, changes caused in the density distribution of the initial system are examined. Possible repercussions of the end state of the system for the star formation process are also discussed.

2 METHOD OF ANALYSIS

In our study of the dynamics of clumps within molecular clouds, we adopt the following simplifying assumptions. A molecular cloud is presumed to consist of two distinct components, one being the high-density clumps and the other the tenuous interclump medium (hereafter abbreviated as ICM). The volume filling fraction for clumps in a molecular cloud, derived from the average densities of the clumps and the entire cloud, is generally of the order of a few per cent (e.g. Blitz & Thaddeus 1980; Pérault, Falgarone & Puget 1985) or much less (Falgarone & Phillips 1991). In view of these observational facts, we believe that our assumption is not too unrealistic. The clumps have therefore been modelled as spherical particles moving through a fluid. This implies that the density fall-off between the clumps and the ICM in our treatment is much sharper than what is observed. The ratio of mass contained in the clumps and ICM is varied (from 10 to 50 per cent) in the different cases, although in general it is assumed that a significant amount of the cloud mass is contained in the interclump gas.

The cloud is assigned spherical symmetry for simplicity, and two states for the gas distribution are considered, one of uniform density and the other a Plummer density profile (cf. Lada, Margulis & Dearborn 1984). For a Plummer distribution, the gravitational potential and the density are given by

$$\Phi(r)=\frac{\Phi_0}{[1+(r/r_0)^2]^{1/2}}, \qquad \rho(r)=\frac{\rho_0}{[1+(r/r_0)^2]^{5/2}}, \tag{1}$$

where r is the distance from the centre of the cloud and r_0 the width of the distribution (here chosen equal to the cloud radius). For the clumps within molecular clouds, the mass spectrum is generally a power law with the power-law exponent x, which is observationally found to vary from 1.1 to 1.7, but is typically about 1.5 (Sanders, Scoville & Solomon 1985; Loren 1989; Stutzki & Güsten 1990). For clumps in the collapse phase and forming stars, the spectrum may be closer to the Salpeter mass function with an index of 2.35. We have adopted the above mass spectrum for the clumps with an index of 2.35 for all our cloud systems, with the exception of one system for which we have varied x to study any dependences on the form of the mass function assumed. The upper and lower cut-offs of the mass spectrum have been appropriately chosen for clouds of different total masses.

First, the system is allowed to evolve under only the gravitational forces arising from the gas and the clumps. About 100 (typically) clumps with masses according to the mass spectrum are integrated over time. The potential arising from the gas is derived from the assumed density distribution described earlier, and the corresponding force obtained. The force acting on a clump, due to all other clumps, is obtained by a simple clump–clump approach, i.e. summing over individual force terms. The potential is softened using a softening parameter equal to the characteristic size of a clump. We have not included clump–clump collisions, for simplicity. The clumps are initially (at $t=0$) given random positions, so that the total configuration corresponds to that of a uniform number density distribution of clumps. The initial velocities for the clumps have their virial values, and are given random orientations. The equations are solved consistently in three dimensions using a fourth-order Runge–Kutta method with adaptive step-size control. Integration times are typically of the order of the cloud lifetime, which is about 50 Myr for molecular clouds in the Galaxy.

In order to study the effects of dynamical friction drag on the clumps, the above analysis is repeated, including the frictional force. The equations of motion are again set up and the forces considered to be acting on an individual clump are the gravitational force due to the cloud gas, clump–clump gravitational interactions and a dynamical drag force due to the ambient gas, along with an increase in mass of the clumps because of accretion. Thus

$$\boldsymbol{F}_{\rm tot}=\boldsymbol{F}_{\rm gas}+\boldsymbol{F}_{\rm clump}+\boldsymbol{F}_{\rm drag}, \tag{2}$$

where the gravitational term due to gas and clumps is determined as above. The drag force is due to the dynamical friction acting on the clump as a result of the gas (Chandrasekhar 1943), and is caused by a density asymmetry of the gas in the wake of the moving clump which tends to retard its motion by exerting a gravitational pull on the clump. The drag is given by (Binney & Tremaine 1987)

$$\boldsymbol{F}_{\rm drag}(r)=\frac{-4\pi\ln\Lambda\, G^2\rho(r)M^2}{v^3}\left[\operatorname{erf}(X)-\frac{2X}{\sqrt{\pi}}\exp(-X^2)\right]\boldsymbol{v}, \tag{3}$$

where $\boldsymbol{v}$ is the velocity of the clump, G is the gravitational constant, M is the mass of the clump, ρ is the density of the gas and $\ln\Lambda$ is the Coulomb logarithm, Λ being equal to the ratio of maximum and minimum impact parameters. (The maximum impact parameter $b_{\rm max}\sim R$, the radius of the cloud, and the minimum impact parameter $b_{\rm min}=GM/v^2$, so that $\Lambda\sim Rv^2/GM$.) The gas velocity distribution is assumed to follow a Maxwellian distribution with a dispersion σ, and X is a dimensionless parameter equal to $v/(\sqrt{2}\sigma)$. Although equation (3) was derived for point particles, it is found to be a reasonably good approximation for extended objects as well, if $r_{\rm c}\lesssim b_{\rm max}/\sqrt{\Lambda}$, where $r_{\rm c}$ is the radius of the object (Binney & Tremaine 1987, p. 426). The velocity dispersion of the gas is taken as equal to the virial velocity for the cloud ($\sigma^2=GM_0/R$, where M_0 is the cloud mass and R its radius). Further, the clump accretes mass from the surrounding medium as it moves with a relative velocity v through the gas at a rate

$$\frac{{\rm d}M}{{\rm d}t}\simeq\pi r_{\rm eff}^2\rho(v^2+\sigma^2)^{1/2}, \tag{4}$$

where $r_{\rm eff}$ is the effective radius of the clump. An increase in mass due to accretion also causes a deceleration, which is equivalent to a gas drag given as

$$\boldsymbol{F}_{\rm gas\,drag}\simeq-\boldsymbol{v}\frac{{\rm d}M}{{\rm d}t}\simeq-\pi r_{\rm eff}^2\rho(v^2+\sigma^2)^{1/2}\boldsymbol{v}. \tag{5}$$

This drag has also been included in the equations of motion. For a clump with a gravitational cross-section larger than its physical cross-section, $r_{\rm eff}$ is given by the gravitational radius $r_{\rm g}=2GM/(v^2+\sigma^2)$. For larger clumps,

$$r_{\rm eff}^2=r_{\rm c}^2\left(1+\frac{r_{\rm g}}{r_{\rm c}}\right), \tag{6}$$

with $r_{\rm c}$ being the physical radius of the clump for accretion. Clumps that are in virial equilibrium, or those that are pressure-confined in GMC complexes and GMCs, usually have relatively large radii ($r_{\rm c}>r_{\rm g}$), and $r_{\rm eff}$ is given by equation (6). The actual accretion process in this case is, however, ill-understood, as the clumps move supersonically through the ambient medium and the formation of bow shocks may prevent any real accretion (Pumphrey & Scalo 1983). Further, any matter impinging on the surface of the clump may cause ablation of the clump rather than be accreted (Scalo & Struck-Marcell 1984). There is, however, transfer of momentum, and the clumps suffer a hydrodynamical drag given by equation (5). From equations (4)–(6), for typical velocities $v\sim\sigma$ the ratio between dynamical friction $F_{\rm d}$ and hydrodynamical drag $F_{\rm gas\,drag}$ is $\sim 0.8\ln\Lambda(r_{\rm g}/r_{\rm c})^2/[1+(r_{\rm g}/r_{\rm c})]$. Thus $F_{\rm gas\,drag}>F_{\rm d}$ for clumps with $r_{\rm c}/r_{\rm g}\gtrsim 0.9\sqrt{\ln\Lambda}\gtrsim 2$ for $\ln\Lambda\sim 5$. The dynamics of such clumps in molecular clouds is dominated by hydrodynamical drag and clump–clump collisions (Scalo & Pumphrey 1982; Elmegreen 1985). Protostellar clumps and protostars are denser objects with $r_{\rm c}<r_{\rm g}$, and the accretion rate is given by (cf. Hoyle & Lyttleton 1939)

$$\frac{{\rm d}M}{{\rm d}t}=\frac{4\pi G^2\rho(r)M^2}{(v^2+\sigma^2)^{3/2}}. \tag{7}$$

We restrict our analysis to protostellar clumps, whose physical radii are smaller than their gravitational radii. The initial masses, positions and velocities of the clumps are assigned in a similar manner to the case for no drag. The masses of the clumps are distributed according to the mass spectrum as before, and the equations are solved. In our model, for simplicity, we have not considered the effects of magnetic fields or collisions between clumps.

3 RESULTS AND DISCUSSION

The formulation described above has been used to obtain the temporal evolution of the protostellar clumps in molecular clouds for a range of parameters. The densities, masses, sizes, etc., have been taken to be similar to those observed for the systems under consideration. The densities and fraction of mass contained in the clumpy form have been varied along with a change in mass spectrum of clumps. In all, 13 cases have been run, and in each individual case the spatial positions and velocities of the constituent clumpy particles have been followed at different epochs of time as the system evolves.

Depending on the prevailing physical conditions, the cloud evolutionary properties change, as is to be expected. The effects of dynamical relaxation of the clumps in a cloud in the presence of a constant gas potential have been looked at first, and it is found that mass segregation due to N-body relaxation takes a long time to be established. The inclusion of the dynamical drag on the clumps significantly alters the dynamics in all the interstellar cloud systems considered, and mass segregation is established in a much shorter time. The dynamical drag acting on a clump is dependent on its mass, and thus clumps of different masses have in general different retardations. The most massive clumps suffer the maximum decelerating effects, and their orbits get closer to the cloud centre. The 'infall' time-scale over which the clump falls to the centre of the cloud is different for clumps of different masses. The more massive clumps settle to the centre in a shorter time than do the lower mass clumps. There is a clustering of the clumps towards the centre of the cloud, and a radial segregation of mass is established in the cloud. This can be seen from the plots in Figs 1 and 2. The clump mass spectrum is divided into logarithmic mass intervals and the masses of the clumps in each such bin are averaged to obtain

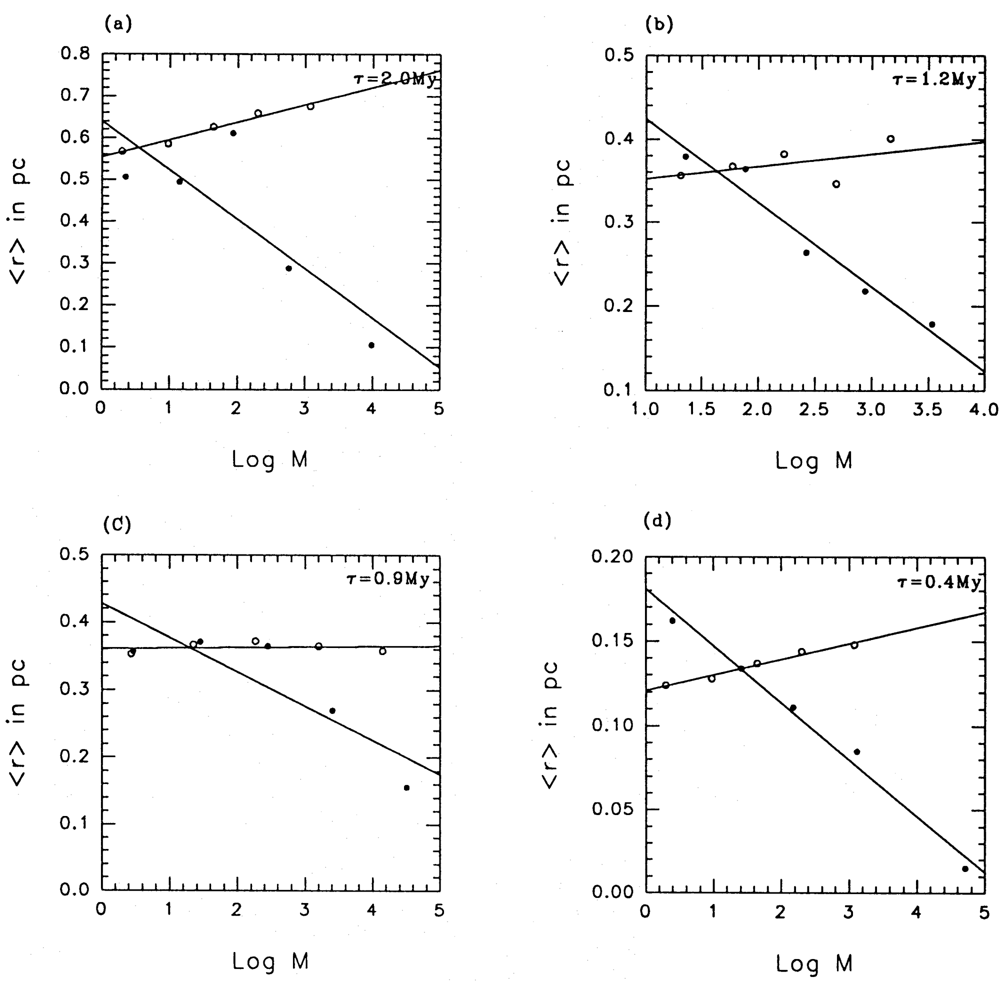

Figure 1. The average positions of clumps, which have been divided into logarithmic mass bins, have been plotted against the mean mass of each bin. The open circles correspond to the initial distribution of the clumps and the filled circles to the distribution after a time τ, indicated in the upper right-hand corner of each plot. Least-squares fits to the points have been drawn. Panels (a), (b), (c) and (d) correspond to clouds I, II, III and IV with increasing average densities of 10^4, 1.2×10^5, 4×10^5 and $10^6\ cm^{-3}$ respectively.

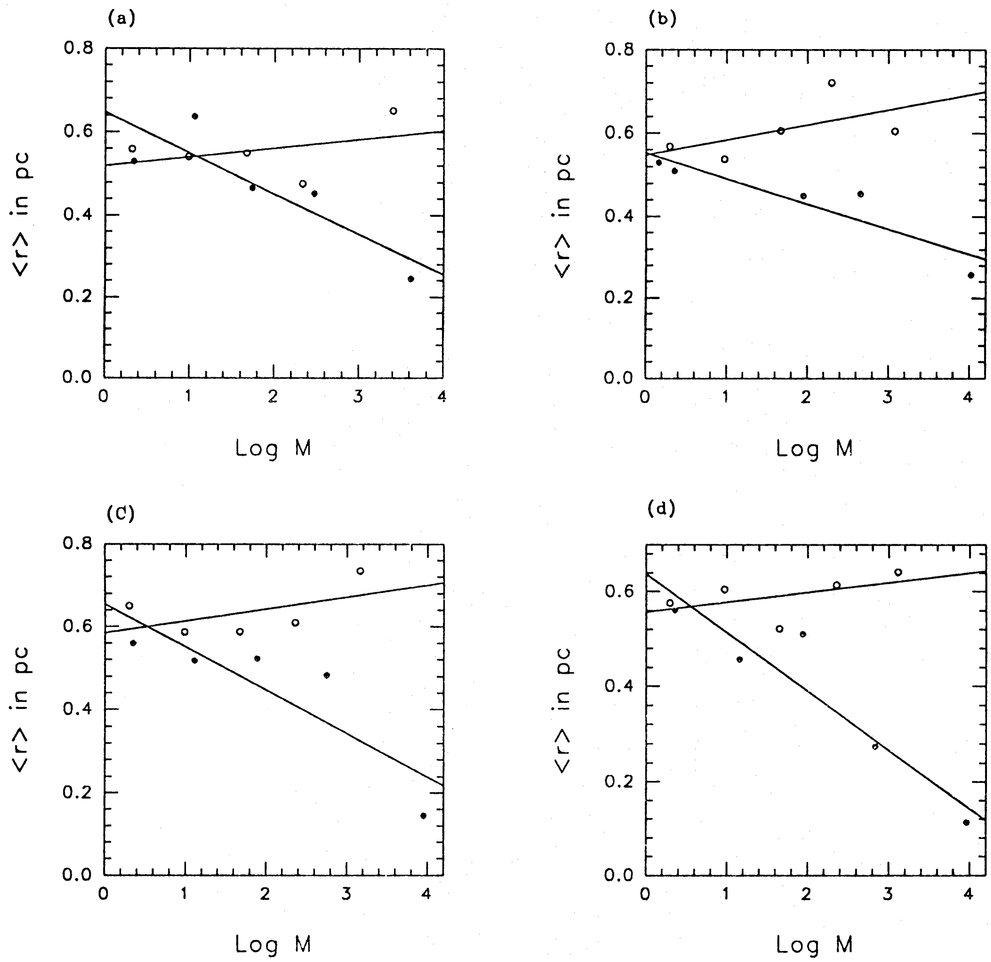

Figure 2. The same conventions as Fig. 1, with the plots corresponding to varying mass fractions of clumps in the cloud (at 2 Myr). Panels (a), (b), (c) and (d) have clump mass fractions of 10, 20, 30 and 50 per cent respectively.

a mean mass for the bin. The positions of the clumps with respect to the cloud centre for each mass bin are similarly averaged to get an average position $\langle r \rangle$, which is plotted against the mean logarithmic mass of the bin. The open and filled circles in the figure correspond to the times $t=0$ and a later time at which the cloud shows evidence of mass segregation. The lines are least-squares fits to the points. Initially, the clumps are distributed over the cloud randomly, and hence all have equal probability of lying anywhere in the cloud, independent of their masses. At later times, the more massive clumps suffer greater drag due to dynamical friction and move towards the centre of the cloud. The least massive clumps, which are not significantly impeded by the drag force, move in orbits that could be located anywhere in the cloud, and thus have an average radial position further from the cloud centre than do the high-mass clumps. This results in a gradual steepening of the slope in the log M–$\langle r \rangle$ plots with time. The time-scale of the process is governed by the cloud parameters, and is shorter for denser clouds. We define a mass segregation time $\tau_{\rm ms}$ in the following manner. The ratio η of the average radial distance $\langle r_{\rm h} \rangle$ of the most massive clumps (in number, 10 per cent of the total population) and that of the least massive clumps $\langle r_{\rm l} \rangle$ has been computed at various times (where $\eta = \langle r_{\rm h} \rangle / \langle r_{\rm l} \rangle$). At $t=0$, η is roughly equal to one, and $\tau_{\rm ms}$ has been considered as the time at which $\eta \simeq 0.5$. It is found that the segregation time-scale $\tau_{\rm ms}$ is typical of the order of a few times the cloud crossing time-scale $\tau_{\rm cross}$ ($\tau_{\rm cross} \sim 2R/\sigma$, where R is the radius of the cloud and σ the velocity dispersion). Figs 1 and 2 show the mass–radius plots for the various systems. As the system further evolves, i.e. at times $t > \tau_{\rm ms}$, there is an expansion of the system, as N-body interactions take some of the low-mass clumps into orbits with radial distances larger than their original radii, and mass segregation is enhanced. Changes in the dynamical evolution of the protostellar clumps with changes in cloud density, mass fraction in the form of clumps, clump mass spectra, and density profile of the inter-clump medium are studied by varying these parameters individually, keeping all others fixed. These cases are discussed below in detail.

3.1 Effect of change in density

Molecular clouds are observed to have a range of densities, from the less-dense warm GMCs to the cool, dense dark clouds, with the star-forming ρ Oph cloud core being a prototypical example of the latter. The effects of a change in the average density of a cloud on the dynamics of its constituent clumps are studied. Four different cases identified as clouds I, II, III and IV are considered, with average densities ranging from 10^4 to 10^6 cm^{-3}. Cloud I has a mass of 10^3 M$_\odot$ and a size of 1.6 pc (velocity dispersion $\sigma_v = 2.3$ km s^{-1}). The average density of the cloud is 10^4 cm^{-3}, and it has 42 per cent of its mass distributed in 150 clumps whose masses range from 1 to 30 M$_\odot$. The ordinary *N*-body dynamical relaxation time for all four cases is greater than 10^7 yr. The spatial mass segregation time-scale is found to be 2.4 Myr, which is far shorter than the ordinary *N*-body relaxation time. Cloud II has a mass of 3×10^3 M$_\odot$, size 1.0 pc, $\sigma_v = 5.1$ km s^{-1} and an average density of 1.2×10^5 cm^{-3}. 185 clumps form 40 per cent of its mass and have masses from 3 to 30 M$_\odot$. Mass segregation takes place on a slightly shorter time-scale of 1.2 Myr. Cloud III ($M = 10^4$ M$_\odot$, $R = 1$ pc, $\sigma_v = 9.3$ km s^{-1}) has an average density of 4×10^5 cm^{-3} and has a segregation time nearly the same as that of cloud II, 0.9 Myr. Cloud IV has the highest average density of 10^6 cm^{-3}. All cloud IV parameters are the same as that of cloud I, except for its size which is 0.25 pc and velocity dispersion ($\sigma_v = 4.9$ km s^{-1}). The mass segregation time-scale is only 0.4 Myr. The mass–radius plots for all four cases are shown in Fig. 1. It should be noted that a density increase by a factor of 100 from cloud I to cloud IV causes a decrease in segregation time-scale by a factor of 6. There is also some expansion of the initial system, as can be seen from Fig. 1. Thus $\tau_{\rm ms}$ is shorter for denser clouds, and segregation effects are expected to be enhanced in the densest star-forming molecular clouds. It seems probable that the mass segregation observed in young star clusters in star-forming regions (e.g. NGC 2071 and 2024: Lada 1991) is a result of the dynamics of the protostellar clumps from which they form.

In all of the above systems, the physical radius of the protostellar clump, $r_{\rm c}$, is assumed to be small compared to its gravitational radius, $r_{\rm g}$. The *N*-body gravitational force is softened using a parameter ε equal to $10^{-3}R$ (3×10^{15} cm for $R = 1$ pc) for all the clumps. For computational convenience, ε is chosen such that it is larger than the clump radius, but should be small enough to allow close clump–clump encounters. For stars, protostars and protostellar clumps that have developed high-density cores that contain most of their mass, our choice of ε is satisfactory. Protostellar clumps that have just begun to collapse, however, may have $r_{\rm c}$ as large as $r_{\rm g}$. We have therefore run the simulation for a case where ε is set equal to $r_{\rm g}$. Although the segregation time $\tau_{\rm ms}$ does not change, and is 2.4 Myr for both cases, there is still a qualitative difference in the subsequent evolution of the system: there is no expansion of the system, with smaller clumps moving out to radii larger than their initial positions, as all clump–clump encounters are highly softened. It can be seen from Fig. 3 that the protostellar clumps form a more compact system after dynamical evolution. When the clumps collapse to form stars, the resulting cluster in such a case has a higher 'apparent' star-forming efficiency, and may eventually form a bound system (cf. Bally & Lada 1991).

3.2 Effect of change in mass fraction in clumps

The total fraction of mass contained in the clumps is varied for cloud I from 10 per cent to 50 per cent. The number of clumps is modified accordingly, with the same power-law spectrum and upper and lower cut-offs. There is no significant difference in mass segregation time-scales. Fig. 2 shows the mass–radius plots for the clouds at the same epoch. The segregation times for the different cases (of cloud I) are as follows: $f_{\rm c} = 0.1$, $\tau_{\rm ms} = 2.0$ Myr; $f_{\rm c} = 0.2$, $\tau_{\rm ms} = 1.8$ Myr; $f_{\rm c} = 0.3$, $\tau_{\rm ms} = 2.4$ Myr and $f_{\rm c} = 0.5$, $\tau_{\rm ms} = 2.0$ Myr. Clouds with lower clump mass fractions have more gas in the ICM; the gas is also denser, as the total mass and radius of the cloud are kept constant. Clouds with small $f_{\rm c}$ are thus expected to segregate faster. The density change from $f_{\rm c} = 0.1$ to $f_{\rm c} = 0.5$, however, is not large enough noticeably to affect the segregation time-scales. (As was seen above, an increase by a factor of 100 in the density causes a change in the mass segregation time-scale by only a factor of 6.) The lack of any systematic trend in $\tau_{\rm ms}$ with varying $f_{\rm c}$ in our simulations is probably a result of poor statistics along with different initial clump conditions (clump positions and velocities at $t = 0$), especially for low $f_{\rm c}$-values.

3.3 Effect of change in mass spectrum index

A change in the exponent of the power-law mass spectrum has only a minor effect on the dynamics of the protostellar clumps. In order to investigate the effect of variation in the

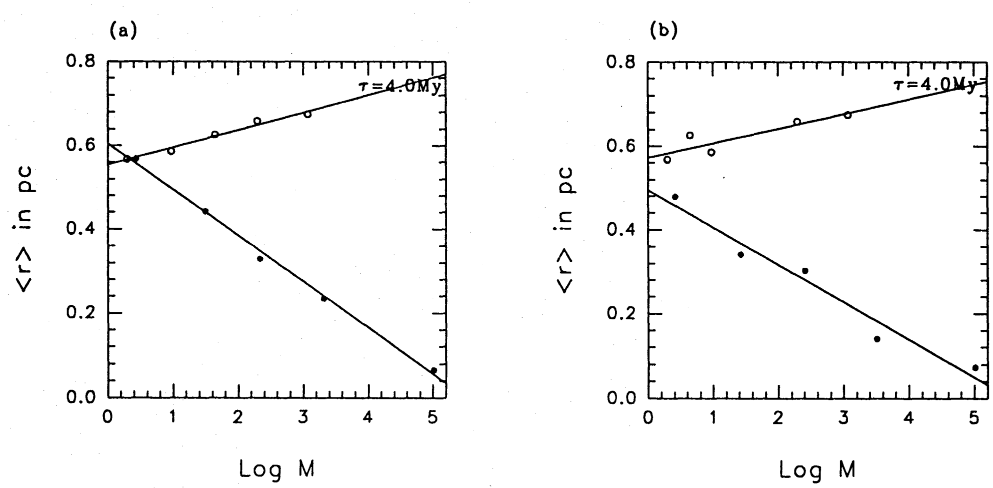

Figure 3. The radial position against mass for cloud I (see text), with different softenings, at 4 Myr. Panel (a) shows the result when a small physical cross-section is assumed for the clumps, and (b) shows the result when their sizes are set equal to their gravitational radii.

mass spectrum index, one of the above cases (cloud I) has been run for $x=1.1$, 1.5 and 2.0, and the stellar mass spectrum index of 2.35. A variation in the power-law exponent for the clumps does not seem to have a very pronounced effect on the final state of the system ($x=1.1$, $\tau_{ms}=2.4$ Myr; $x=1.5$, $\tau_{ms}=2$ Myr; $x=2.0$, $\tau_{ms}=2$ Myr; $x=2.35$, $\tau_{ms}=2.4$ Myr). In each case, the fraction of the mass contained in the clumps (40 per cent) has been kept constant by suitably adjusting the number of clumps, so that the gravitational potential does not change appreciably. Fig. 4 shows that the extent of segregation (at the same epoch of 2 Myr) is little affected by a change in the mass spectrum. As the clumps accrete gas from the ambient medium at a rate dependent on their masses, the mass spectrum of the clumps could also potentially be altered. Such changes are found to be almost negligible, however, as the accretion rates are not high enough to change the power-law index significantly, in any of the cases considered. The power-law exponent after segregation, x_f, has been computed for the two extreme cases. For $x=1.1$, $x_f=1.15$; for $x=2.35$, x_f is found to be 2.31.

3.4 Effect of a change in the density distribution of the ICM

The density distribution of the gas, i.e. the interclump medium, for all of the above clouds is given by the Plummer distribution (equation 1). The analysis for cloud I has been repeated for a constant density or a uniform gas distribution, to study any alterations brought about by variations in the gas density profile. The same initial conditions have been imposed, and it is found that the mass segregation time-scale increases (Figs 5a and b) marginally. A steepening in the density profile of the cloud due to mass segregation is also found, as is to be expected, especially when the clumps form a significant fraction of the total mass.

As a result of the drag forces acting on the clumps, there is a spatial mass segregation established in the molecular cloud clumps. The velocity distribution is also affected. The protostars are acted upon by dynamical friction as they move through the cloud. They are decelerated and their orbits get closer to the cloud centre. They tend to approach local virial velocities at their new positions. Decay of the orbits of the

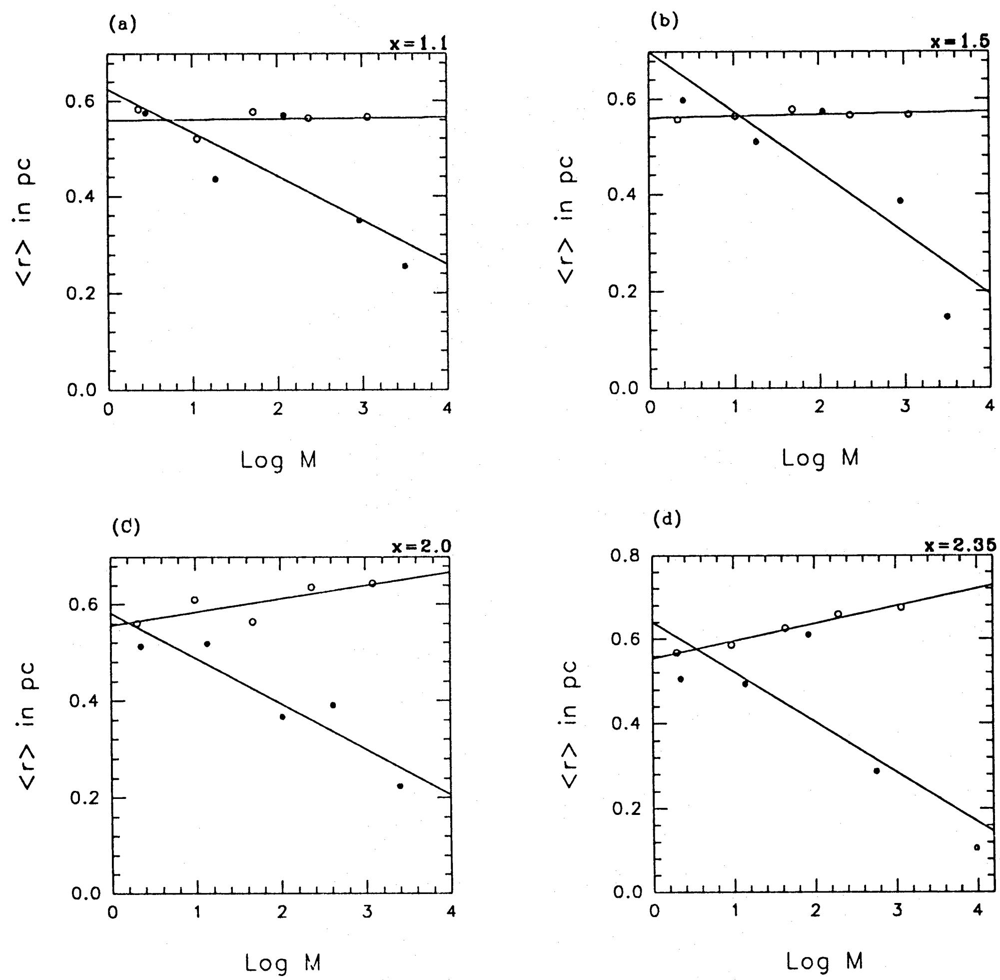

Figure 4. These plots show average position against mass for clouds with the same parameters, but with different mass spectra for the clumps. They are all at the same epoch (2 Myr) and the mass spectrum power-law exponent is denoted by x, shown in the upper right-hand corner for each case.

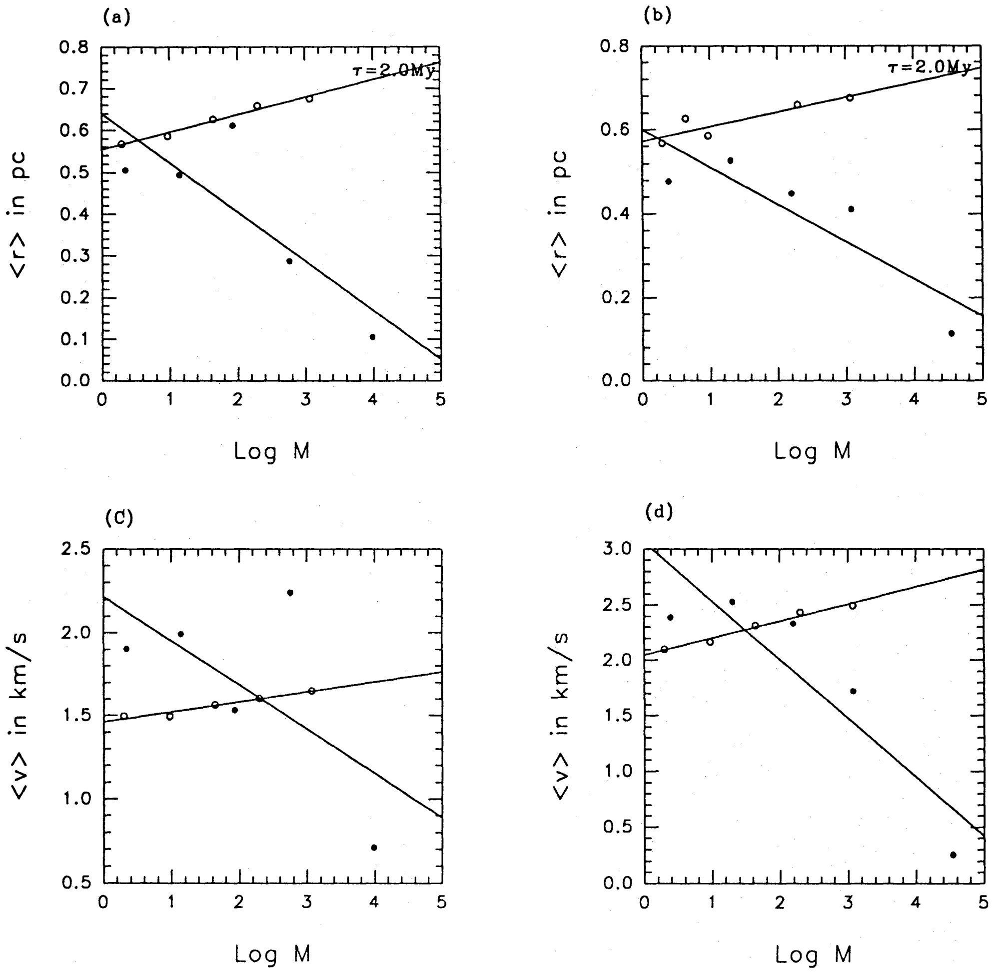

Figure 5. Variations in the extent of mass segregation with respect to the density profile of the interclump gas. A constant density cloud and a Plummer model are considered. Panels (a) and (b) show the extent of spatial mass segregation, and (c) and (d) show the velocity dispersion against the mean logarithmic mass of each bin. The open circles and fitted lines correspond to the initial times, and the filled circles to a time of 2 Myr.

most massive protostars also modifies the density structure in the inner regions of the cloud, which in turn causes a change in the virial velocities in this region. For a power-law density profile of the form $\rho(r) \propto r^{-\alpha}$, the virial velocity is given by $v(r) \propto r^{(-\alpha+2)/2}$. Thus the velocity dispersion increases with increasing radius for a cloud with a density profile less steep than $\alpha = 2$. Such clouds are expected to show a velocity segregation with mass along with the spatial mass segregation, whereas clouds with steeper density profiles are likely to show an increase in velocity dispersion towards the centre of the cloud. This increase could, to some extent, compensate the loss due to drag, thus decreasing the extent of segregation of mass with respect to velocity. Figs 5(c) and (d) show the velocity dispersion against log M for the constant density and Plummer density models, respectively. Velocity segregation with respect to mass is more apparent for the constant density model than for the Plummer model.

Thus mass segregation appears to be an inevitable consequence of clump dynamics in most interstellar clouds. For a thorough analysis of the cloud–clump systems, all the forces acting on the clumps have to be included, in particular clump–clump collisions and magnetic field effects. Collisions are expected to be important, especially after a central clustering of clumps has occurred, if not at an earlier stage. The outcome of a collision depends on the parameters of the encounter, and in general could lead to either a coalescence of the clumps to form a larger clump, or a fragmentation into smaller clumps. If it is assumed that collisions cause clumps to coalesce, we can conclude that the massive clumps thereby formed will lose momentum and sink to the centre of the cloud. This will also lead to spatial segregation of mass in the cloud. We make simple estimates of the time-scales involved in collisional and drag processes for comparison, as follows. The time-scale over which dynamical friction causes deceleration can be obtained from equation (3) for the drag force, and can be written as

$$\tau_{\rm drag} \simeq \frac{v^3}{4\pi \ln \Lambda\, G^2 M \rho [\mathrm{erf}(X) - 2X \exp(-X^2)/\sqrt{\pi}]}. \tag{8}$$

The time-scale for deceleration of a clump due to clump–clump collisions will be of the order of the time-scale for the growth of the clump mass due to accretion of clump masses, following collisions that result in coalescence. The rate of change of mass of a clump due to collisions and subsequent coalescence can be approximated as an effective cross-sectional area times a mass flux:

$$\frac{\mathrm{d}M}{\mathrm{d}t} \simeq \pi r_{\mathrm{eff}}^2 \langle \rho_{\mathrm{c}} \rangle v_{\mathrm{rel}}, \tag{9}$$

where r_{eff} is given by equation (6) and ρ_{c} is the mass density in the form of clumps, arranged over the volume of the cloud. The relative velocity of the encounter is denoted by v_{rel}, which is of order $\sqrt{2}v$. The collisional time-scale τ_{coll} is given by $M/(\mathrm{d}M/\mathrm{d}t)$, and the ratio of the two time-scales can be written as

$$\frac{\tau_{\mathrm{drag}}}{\tau_{\mathrm{coll}}} \simeq 1.3 \frac{\rho_{\mathrm{c}}}{\rho \ln \Lambda} \left(\frac{r_{\mathrm{eff}}}{r_{\mathrm{g}}} \right)^2. \tag{10}$$

Thus collisional drag dominates dynamical friction only when

$$\frac{r_{\mathrm{c}}}{r_{\mathrm{g}}} \gtrsim 0.9 \sqrt{\frac{\rho}{\langle \rho_{\mathrm{c}} \rangle} \ln \Lambda}. \tag{11}$$

Typically, $\rho \sim \rho_{\mathrm{c}}$ and $\ln \Lambda \sim 5$. Thus, for the situations under consideration here with $r_{\mathrm{c}} < r_{\mathrm{g}}$ $(r_{\mathrm{eff}} = r_{\mathrm{g}})$, the drag time is much shorter than the collision time and mass segregation due to drag dominates that due to collisions, by a factor of ~ $0.9 \ln \Lambda$. Collisions may considerably affect the dynamics at the centre of the cloud, however, where the number density is enhanced by drag effects. If the outcome of a collision is fragmentation rather than a coalescence, the evolution may be quite different. For a more realistic picture, a detailed model of the collision process has to be made and included with the gas drag to study the motions of the clumps within the cloud.

The magnetic field in clouds is an important contributor to the overall energy density of the cloud, and doubtless has an important role to play in governing the dynamics of the clumps, more so if the principal mode of support in the cloud against gravitational collapse is magnetic pressure. The subject of the inclusion of magnetic fields is, however, beyond the scope of the present work. Although the consequences of the drag force acting on the clumpy constituent of the molecular cloud seem to hold an interesting variety of possibilities, it should be noted that the present treatment is very simplistic and that, for a more realistic analysis, collisions and magnetic fields have to be taken into account.

4 CONCLUSIONS

Protostellar clumps moving in molecular clouds through an ambient interclump medium are acted upon by the decelerating forces of dynamical drag due to the gas, lose momentum and fall towards the centre of the cloud. Since the forces are mass-dependent, the more massive clumps suffer greater drag and settle towards the centre on shorter time-scales. This causes a radial segregation with respect to mass of the clumps in the cloud. This segregation induced by dynamical friction is found to be significant for protostellar clumps in interstellar clouds, as the time-scale involved is much shorter than the typical cloud lifetime or the *N*-body relaxation time. The segregation is more pronounced and quicker in denser clouds. Variations in clump mass spectra and the density profile of interclump gas have little effect on the dynamics, and do not greatly affect the time-scale of segregation in the cloud system. The fractions of mass contained in the clumpy and tenuous forms to some extent influence the dynamics of the system, but the segregation time-scales are not significantly altered. There is also some velocity segregation with respect to mass, with the more massive clumps tending to have lower velocities. This is not, however, as pronounced as the radial segregation. The most massive star-forming clumps are thus expected to be closer to the centre of the parent cloud. Subsequent star formation in these clumps could then explain the mass segregation observed in many young clusters of pre-main-sequence stars and young stellar objects.

ACKNOWLEDGMENTS

We thank Professor I. P. Williams for stimulating discussions during the early stages of this work. We also thank the referee, Professor B. Elmegreen, for many useful suggestions.

REFERENCES

Bally J., Lada E., 1991, in Janes K. A., ed., ASP Conf. Ser. Vol. 11, The Formation and Evolution of Star Clusters. Astron. Soc. Pac., San Francisco, p. 38
Bally J., Langer W. D., Stark A. A., Wilson R. W., 1987, ApJ, 312, L45
Beichman C. A., Myers P. C., Emerson J. P., Harris S., Mathieu R., Benson P. J., Jennings R. E., 1986, ApJ, 307, 337
Binney J., Tremaine S., 1987, Galactic Dynamics. Princeton Univ. Press, Princeton, NJ
Blitz L., 1991, in Lada C. J., Kylafis N. D., eds, The Physics of Star Formation and Early Stellar Evolution. Kluwer, Dordrecht, p. 3
Blitz L., Stark A. A., 1986, ApJ, 300, L89
Blitz L., Thaddeus P., 1980, ApJ, 238, 148
Chandrasekhar S., 1943, ApJ, 97, 255
Elmegreen B. G., 1985, ApJ, 299, 196
Falgarone E., Phillips T. G., 1990, ApJ, 359, 344
Falgarone E., Phillips T. G., 1991, in Falgarone E., Boulanger F., Duvert G., eds, Fragmentation of Molecular Clouds and Star Formation. Kluwer, Dordrecht, p. 119
Falgarone E., Puget J. L., 1988, in Pudritz R., Fich M., eds, Galactic and Extragalactic Star Forming Regions. Kluwer, Dordrecht, p. 195
Falgarone E., Phillips T. G., Walker C., 1991, ApJ, 378, 196
Genzel R., 1991, in Lada C. J., Kylafis N. D., eds, The Physics of Star Formation and Early Stellar Evolution, p. 230
Genzel R., 1992, in Burton W. B., Elmegreen B. G., Genzel R., eds, The Galactic Interstellar Medium. Springer-Verlag, Berlin, p. 353
Hoyle F., Lyttleton R. A., 1939, Proc. Camb. Phil. Soc., 35
Lada E., 1990, PhD thesis, University of Texas
Lada C. J., 1991, in Lada C. J., Kylafis N. D., eds, The Physics of Star Formation and Early Stellar Evolution, p. 339
Lada C. J., Margulis M., Dearborn D., 1984, ApJ, 285, 141
Larson R. B., 1982, MNRAS, 200, 159
Loren R. B., 1989, ApJ, 338, 902
Myers P., 1987, in Peimbert M., Jugaku J., eds, Proc. IAU Symp. 115, Star Forming Regions. Reidel, Dordrecht, p. 33
Pérault M., Falgarone E., Puget J. L., 1985, A&A, 152, 371
Pumphrey W. A., Scalo J., 1983, ApJ, 269, 531
Sanders D. B., Scoville N. Z., Solomon P. M., 1985, ApJ, 289, 373

Scalo J., 1990, in Capuzzo-Dolcetta R., Chiosi C., deFazio A., eds, Physical Processes in Fragmentation and Star Formation. Kluwer, Dordrecht, p. 151
Scalo J., Pumphrey W. A., 1982, ApJ, 258, L29
Scalo J., Struck-Marcell C., 1984, ApJ, 276, 60
Stutzki J., Güsten R., 1990, ApJ, 356, 513
Tatematsu K. et al., 1993, ApJ, 404, 643
Wilson T. L., Walmsley C. M., 1989, A&AR, 1, 141